Hindawi
Journal of Clinical Pharmacy and Therapeutics
Volume 2023, Article ID 4837743, 10 pages
https://doi.org/10.1155/2023/4837743

Research Article

Exploration of the Mechanism of Valsartan Treatment in Chronic Renal Failure: Network Pharmacology and Experimental Validation

Min Zhu,[1,2] Zhaoran Wang,[3] Ziming Zhu,[2] Cuifeng Zhang,[3] and Fanrong Wu [1]

[1]*School of Pharmacy, Anhui Medical University, Hefei 230032, China*
[2]*Department of Pharmacy, Xuancheng People's Hospital, The Affiliated Xuancheng Hospital of Wannan Medical College, Xuancheng 242000, China*
[3]*School of Anesthesiology, Wannan Medical College, Wuhu 241000, China*

Correspondence should be addressed to Fanrong Wu; aydwfr@163.com

Received 13 March 2023; Revised 10 August 2023; Accepted 7 September 2023; Published 16 October 2023

Academic Editor: Keiko Hosohata

Objective. To investigate the targets and mechanisms of valsartan in the treatment of chronic renal failure based on network pharmacology and animal experiment validation. *Methods*. The objectives of using valsartan were predicted with the PubChem and SwissTargetPrediction databases. Relevant targets of chronic renal failure have been searched in various disease databases, with the common purposes of drugs and diseases extracted. Network analysis was carried out with the STRING database to construct a protein-protein interaction (PPI) network, as Cytoscape 3.9.1 software was used to analyze network topology of the key targets and establish the "valsartan-core target gene" network. Gene Ontology (GO) and the Kyoto Encyclopedia of Genes and Genomes (KEGG) enrichment analyses were performed on core targets to explore their possible molecular mechanisms. The chronic renal failure mouse model was established by the plat method. Hematoxylin-eosin (H&E) and Masson staining observed morphological changes in renal problems of each group, as levels of serum Cre, BUN, T-SOD, and MDA in each group were detected by kit; real-time PCR was used to detect the relative expression of mRNA of TNF-αIL-1β, IL-6, and IL-10 in renal disease of mice in each group, with WB detect CALM, PKCα, and CaMKIV protein expression levels in renal disease from each group. *Results*. The network pharmacology approach identified 10 key targets for treatment of chronic renal failure with valsartan, including EGFR, PTGS2, PPARG, and ERBB2. KEGG enrichment analysis predicted that the drug exerted neuroactive ligand-receptor interaction, the calcium signaling pathway, the HIF-1 signaling pathway, the proteoglycans in cancer, PD-L1 expression, and the PD-1 checkpoint pathway in cancer. Results from animal experiments were compared to those of the model group, as renal function was significantly improved in the valsartan-dose group. The serum levels of Cre, BUN, and MDA and relative mRNA expression of TNF-α, IL-1β, and IL-6 decreased significantly, while serum T-SOD levels, relative mRNA expression of IL-10, and the protein expression level of CALM, PKCα, and CaMKIV increased significantly ($P < 0.05$ and $P < 0.001$). *Conclusion*. Valsartan yields certain renal protection, which may improve chronic renal failure in mice through the calcium signaling pathway.

1. Introduction

Kidney disease and associated complications have now become an important global public health problem. In recent years, the number of patients with end-stage renal disease in China has increased rapidly and will continue to increase in the next few years [1, 2]. Though chronic kidney disease (CKD) is caused by many factors, good blood pressure control prevents progression of CKD [3], which is closely related to the incidence of end-stage renal disease (ESRD) and the mortality of cardiovascular disease (CVD) [4, 5]. With an increasing prevalence of CKD and a lack of effective treatment, this has caused serious health problems worldwide [6, 7].

Studies found that valsartan has a lasting and stable blood pressure effect and few toxic side effects, especially for secondary hypertension caused by renal damage, and can

reduce the mortality of heart patients with left ventricular dysfunction [8]. In addition, valsartan can weaken platelet activity by attenuated COX-2/TXA2 expression through p38-MAPK and NF-κB pathways and reduce cardio thrombotic events in elderly hypertensive patients [9]. Since there is no specific clinical treatment plan for CKD, it is urgent to improve patients' symptoms and find effective and safe therapeutic drugs for them. As such, in this study, the network pharmacology method was used to predict potential key targets and related molecular pathways of valsartan in treating chronic renal failure, which were validated by animal experiments, as well as clarifying the role of valsartan in improving the development of chronic renal failure, and finding preventive and treatment drugs for treatment of hypertension combined with chronic renal failure. We elucidated the role of valsartan in improving chronic renal failure to then find effective prevention drugs for clinical treatment of hypertension, combined with chronic renal failure.

2. Materials and Methods

2.1. Materials. Experimental reagents used were as follows: valsartan (H20040217, Novartis); GAPDH (60004-1-Ig, Proteintech); CALM (AF1435, Beyotime); PKCα (AF1576, Beyotime); CaMK (WL04335, Wanleibio); SDS-PAGE fast-gel kit (P0012A, Beyotime); HRP-labeled Goat Anti-Rabbit IgG (H + L)(A0208, Beyotime); HRP-labeled Goat Anti-Mouse IgG (H + L)(A0216, Beyotime); ECL chemiluminescence kit (P90719, Millipore); RIPA (strong) lysate (P0013B, Beyotime); urea nitrogen (BUN) test box (C013-2-2, Nanjing Jiancheng); creatinine assay kit (C011-2-1, Nanjing Jiancheng); total superoxide dismutase activity colorimetric assay kit (A001-1-2, Nanjing Jiancheng); and micromalondialdehyde (MDA) assay kit (A003-2-2, Nanjing Jiancheng).

Laboratory animals at 6–8 weeks SPF grade, adult healthy C57BL/6 male mice, weighing 18 – 22 g, were purchased from GemPharmatech Co., Ltd (Nanjing, China), animal production license No. SCXK (Su) 2020-0004. All experimental mice maintained a biological rhythm, a constant temperature and humidity (20–25°C, 45%–75%), and light circadian control (8: 00–20:00), with adaptive feeding for a week.

Experimental instruments used were as follows: high-throughput vertical frozen grinder (MB-LD48, MEBI INSTRUMENTS); fluorescent microplate reader (Spark, Tecan); chemiluminescence analysis system (Tanon5200, Tanonh); ultratrace protein nucleic acid analyzer (Ulite+, BioDrop); real-time PCR instrument (QuantStudio3, Thermo Fisher); and inverted fluorescence microscope (YIB510FL, YUESHI).

2.2. Methods

(i) Potential targets for valsartan: The chemical structure of valsartan was obtained from the PubChem database (https://pubchem.ncbi.nlm.nih.gov/) and imported into component target database SwissTargetPrediction (https://swisstargetprediction.ch/) and TargetNet (https://targetnet.scbdd.com/calcnet/index/). After selecting species as a gene with human *Homo sapiens* and prob > 0, potential targets for valsartan were obtained. Using UniPort (https://www.uniprot.org/) to standardise targets in TargetNet, we merged two databases and removed duplicate targets.

(ii) Target prediction of chronic renal failure: "Chronic renal failure" was searched in the Human Gene database (GeneCards, https://www.genecards.org/), Genetic Pharmacology and Pharmacogenomics database (PharmGKB, https://www.pharmgkb.org), Drug Target database (DrugBank, https://www.drugbank.ca), and Drug Target database (TTD, https://db.idrblab.net/ttd/). After acquiring disease targets of hypertension combined with chronic renal failure, target information from four databases was combined and duplicates were removed.

(iii) The establishment of a PPI network and screening of key targets: By using Venny2.1.0 (https://bioinfogp.cnb.csic.es/tools/venny/index.html), valsartan and chronic renal failure targets were obtained. After overlapping targets and drawing a Wayne diagram, potential targets of valsartan to treat chronic renal failure were taken from the intersection. Resulting intersection targets were uploaded to the STRING 11.5 platform (https://cn.string-db.org/), and "*Homo sapiens*" as the species was qualified. After the PPI network map was constructed for chronic renal failure of the valsartan target, a TSV file was exported and imported into the Cytoscape 3.9.1 software. Ten targets were selected as key targets per degree values (degree).

(iv) GO and the Kyoto Encyclopedia of Genes and Genomes (KEGG) pathway enrichment analyses: In R studio software, we set "p value = 0.05" and "q value = 0.05" and assessed GO and KEGG enrichment for common targets of valsartan/chronic renal failure, drawing corresponding bar or bubble plots.

(v) Molecular docking: The process involved selecting the top 10 active targets based on the degree values from the "valsartan-potential targets-chronic kidney failure" network diagram. The drug compound's sdf format was exported from the PubChem database and subsequently converted to mol2 format using the Open Babel GUI software. The AutoDock software was employed for molecular processing of relevant molecules, encompassing the addition of hydrogens, designation as ligands, torsion angle detection, and torsion bond selection. The crystal protein structures of the top 10 core targets in the protein-protein interaction

Table 1: Primer sequence of real-time PCR.

Name	Forward primer (5′-3′)	Reverse primer (5′-3′)
β-Actin	CGTTGACATCCGTAAAGACC	AACAGTCCGCCTAGAAGCAC
TNF-α	TACTGAACTTCGGGGTGA	ACTTGGTGGTTTGCTACG
IL-1β	GGACAAGCTGAGGAAGATGC	TCGTTATCCCATGTGTCGAA
IL-6	TAGTCCTTCCTACCCCAATTTCC	TTGGTCCTTAGCCACTCCTTC
IL-10	CTTACTGACTGGCATGAGGATCA	GCAGCTCTAGGAGCATGTGG

(PPI) network were retrieved from the RCSB PDB database (https://www.rcsb.org). Subsequently, the Pymol software was utilized to remove water molecules, clear ligands, and save the structures in pdb format. The protein was subjected to hydrogenation using the AutoDock software and then exported in the pdbqt format. The docking parameters and computational methods were set to default values, and the AutoDock program was executed to perform molecular docking, followed by an examination of the docking outcomes. The docking efficacy between active compound ligands and core target protein receptors was evaluated based on their binding energy. The molecular docking outcomes were visualized once more using Pymol. Notably, a higher binding activity between the active compound ligands and the core target protein receptors corresponded to lower binding energy values.

(vi) Laboratory animal modeling and group random number method: The C57BL/6 mice were divided into 5 groups ($n = 5$): the sham group, the model group, the valsartan low-dose group ($10\ mg{\cdot}kg^{-1}$), the valsartan medium-dose group ($20\ mg{\cdot}kg^{-1}$), and the valsartan high-dose group ($50\ mg{\cdot}kg^{-1}$). In the established model of chronic renal failure (CRF), mice in the sham group only exposed the kidney and resutured the wound, while remaining mice used the internationally recognised 5/6 kidney resection surgery (plot method). One week after mold-making, each group of mice received drug gavage as per the experimental protocol. The sham and model groups were given equal volume of CMC-Na solution once a day for 4 consecutive weeks. Mice in each group fasted with water 12 h before specimen collection. After intraperitoneal injection of 3% sodium pentobarbital, blood was collected from the eyes and centrifuged at $5000\ r{\cdot}min^{-1}$ for 15 min, and the supernatant was removed and kept in a −80°C refrigerator. Blood-collected mice were fixed on a sterile operating table, and kidney tissues were harvested, fixed in 4% neutral formaldehyde, dehydrated, and embedded in paraffin, as other tissues were kept in a −80°C refrigerator.

(vii) The histopathological changes in the kidney were observed by hematoxylin-eosin (H&E) and Masson staining. Fixed liver tissues were dehydrated with gradient alcohol and embedded in paraffin. Following the preparation of 3 μm continuous sections, the samples were dewaxed using xylene, subjected to gradient alcohol hydration, and then rinsed with distilled water. Subsequently, conventional H&E and Masson staining were applied. The glomerular disintegration atrophy, inflammatory cell infiltration, renal tubule deformation, collagen deposition, and renal fibrosis of mice renal tissue sections were observed under an optical microscope. We randomly observed 20 fields of each section at high magnification (20x) under a light microscope.

(viii) Serum BUN, Cre, MDA, and T-SOD levels of mice in each group were detected as per the reagent kit (Nanjing Jiancheng Biological Engineering Institute) instructions.

(ix) The mRNA expression levels of related genes in kidney tissue were detected by quantitative real-time polymerase chain reaction (RT-qPCR). We collected partial kidney tissue from mice in each experimental group, performed total mRNA extraction using the Trizol method, employing β-actin as an internal reference gene, and conducted amplification reactions utilizing the Applied Biosystems QuantStudio 3 system. All primer sequences are shown in Table 1.

(x) Western blotting was used to detect expression levels of related proteins in the kidney tissue of each group. Partial mice kidney tissue in each group was added with appropriate RIPA (strong) lysate and homogenized at 60 Hz for 60 s. Total protein in the supernatant was obtained after centrifugation (12,000 rpm) for 10 min. Total protein concentration was determined with an enhanced BCA protein assay kit. Then, 5× protein loading buffer was added, heated at 95°C for 10 min for denaturation, and stored at −20°C. Moreover, 10% SDS-PAGE separation gel was prepared according to the kit. Electrophoresis (constant pressure) was performed at 80 V for 30 min and 120 V for 60 min. Transfer at 300 mA for 90 minutes. We used 5% skim milk powder to prevent nonspecific binding with antibodies (room temperature shaker for 2 h) and washed with 0.1% TBST 3 × 5 min. A primary antibody was incubated at 4°C (1 : 1000) overnight. After washing with TBST 3 times for 5 min per wash, blots were incubated with a horseradish peroxidase-labeled secondary antibody, prepared by adding 5%

skim milk powder (1 : 10000) at room temperature for 60 min. Wash 3 times with 0.1% TBST for 5 min each. Labeled bands underwent a chromogenic reaction using ECL detection reagent and were visualised with a WB luminometer (5,200 multi, Tanon, China). ImageJ software was used for protein gray value analysis.

2.3. Statistical Analysis. SPSS13.0 software was used for statistical analysis. Measurement data were expressed as $(\overline{x} \pm s)$. The t-test compared differences between the two groups, as one-way analysis of variance (ANOVA) was used for comparison between multiple groups. $P < 0.05$ was considered statistically different, $P < 0.01$ was considered a significant statistical difference, and $P < 0.001$ was considered a remarkable statistical difference.

3. Results

3.1. Network Pharmacology Results

(i) Prediction of potential targets for valsartan action: Through the SwissTargetPrediction and TargetNet databases, 25 and 98 potential action targets of valsartan were obtained, respectively. After gene names were unified in a UniProt database, and all chemical components and targets were standardised and merged, with deleted duplicates, a total of 115 effective target genes were obtained.

(ii) Chronic renal failure disease and drug-disease intersection targets: By searching GeneCards, PharmGKB, DrugBank, and TTD, 5,018 human targets related to chronic renal failure were found. After removing duplicate values, a total of 4,901 human targets of chronic renal failure disease were obtained. Moreover, 66 targets common to valsartan and chronic renal failure were extracted using Venny2.1.0 and considered potential core targets for valsartan to treat chronic renal failure (Figure 1(a)).

(iii) The establishment of PPI network and screening of key targets: The 66 common targets were imported into the STRING11.5 database to obtain the PPI network maps (Figure 1(b)). Results exported in TSV format were imported into the Cytoscape software, and key targets were screened according to the degree value, as the top 10 were key targets (Figures 1(c) and 1(d)).

(iv) GO and KEGG pathway enrichment analysis: By GO analysis of the gene ontology database, 1,482 cell components (CC), molecular function (MF), and biological processes (BPs) were enriched for key target genes. They were ranked as per the corrected P value, with the top 8 bars selected for bar chart display (Figure 2(a)). A total of 76 enriched pathways were obtained from the top 20 pathways (Figure 2(b)).

(v) Molecular docking: The core targets, namely, EGFR, PTGS2, PPARG, ERBB2, ACE, STAT3, MMP9, PPARA, PTPRC, and ITGB1, were subjected to molecular docking using the AutoDock software. The protein crystal structures of these core targets were selected from the RCSB PDB database. AutoDockTools were configured to default settings, and each component was hydrogenated before undergoing molecular docking with the respective targets. The results demonstrated that valsartan could effectively dock with EGFR, PTGS2, PPARG, ERBB2, ACE, STAT3, MMP9, PPARA, PTPRC, and ITGB1, yielding favorable docking outcomes. The binding energies were measured as follows: −3.14 kcal/mol for EGFR, −2.77 kcal/mol for PTGS2, −2.6 kcal/mol for PPARG, −3.31 kcal/mol for ERBB2, −1.48 kcal/mol for ACE, −1.52 kcal/mol for STAT3, −4.43 kcal/mol for MMP9, −1.09 kcal/mol for PPARA, −2.08 kcal/mol for PTPRC, and −2.41 kcal/mol for ITGB1 (Figure 3).

3.2. Results of Animal Experiments

(i) Histopathological observation of the mouse kidney in each group: To validate results of network pharmacology, C57BL/6 mice were used to investigate the ameliorating effect of valsartan on chronic renal failure. Compared to the model group, the kidney tissue structure of the valsartan-dose group was basically restored to normal, as the glomerulus and renal interstitium were significantly improved, inflammatory infiltrates and vacuoles decreased significantly, renal collagen fibers decreased, and the degree of fibrosis was significantly improved. In addition, serum creatinine (Cre), urea nitrogen (BUN), and malondialdehyde (MDA) contents were significantly decreased, and total superoxide dismutase (T-SOD) was significantly higher, with statistically significant differences ($P < 0.05$) (Figure 4).

(ii) Analysis of real-time-per results: Compared to the model group, the mRNA expression levels of TNF-α, IL-1β, and IL-6 significantly decreased in renal tissue at each dose of valsartan. The mRNA expression level of IL-10 significantly increased, and the difference was statistically significant ($P < 0.05$) (Figure 5).

(iii) Western blot analysis of results: To further validate the KEGG enrichment analysis, we detected proteins related to the calcium ion signaling pathway. Western blot results showed that protein expression of CALM, PKCα, and CaMKIV in renal tissue of valsartan-dose mice increased significantly ($P < 0.01$ or $P < 0.001$) (Figure 6).

4. Discussion

With acceleration of the aging process in China's population, the number of chronic diseases and deaths is increasing, which threatens the health of our residents [10].

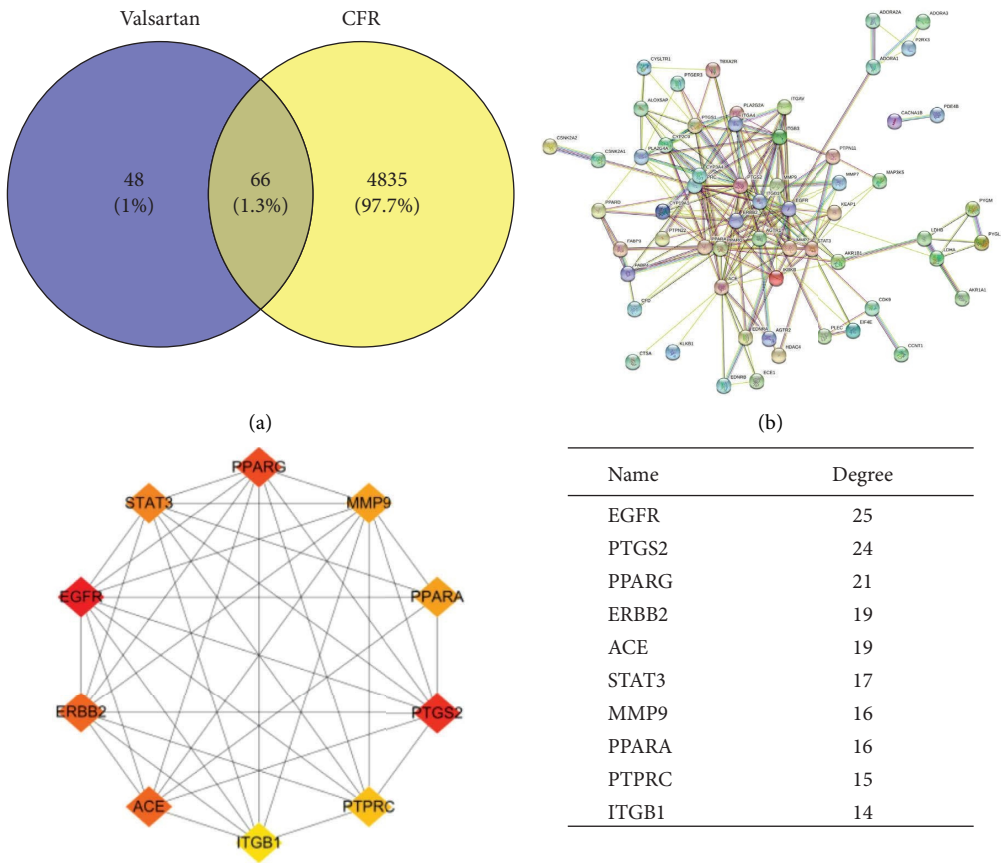

Name	Degree
EGFR	25
PTGS2	24
PPARG	21
ERBB2	19
ACE	19
STAT3	17
MMP9	16
PPARA	16
PTPRC	15
ITGB1	14

(d)

Figure 1: The network pharmacology target search. (a) The target of valsartan and chronic renal failure intersect; (b) the PPI network of valsartan targets for chronic renal failure; (c) core target map of valsartan to treat chronic renal failure; (d) the heat map of the core target in valsartan treated chronic renal failure.

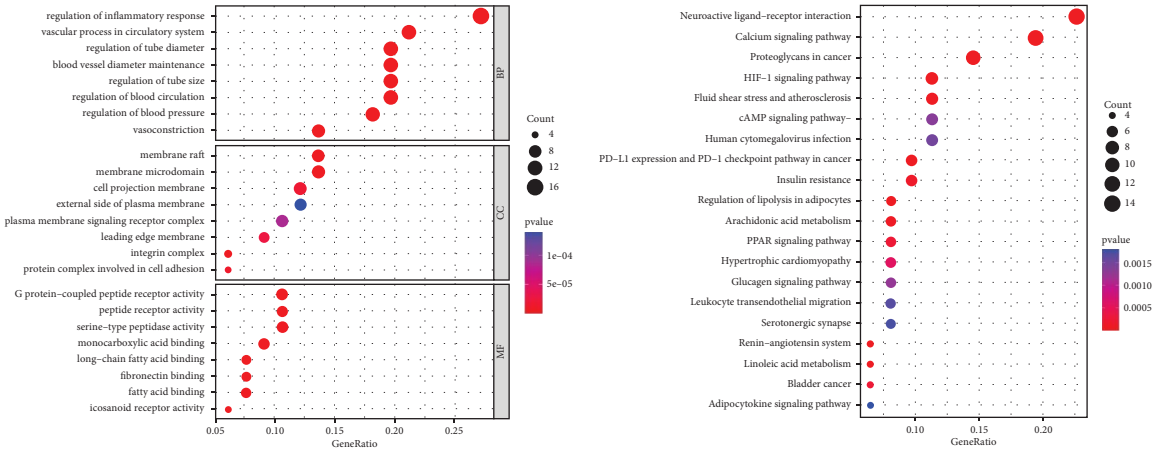

Figure 2: GO and KEGG analysis of key targets of valsartan to treat chronic renal failure. (a) GO enrichment analysis; (b) KEGG enrichment analysis.

Hypertension is one of the most common chronic diseases, accompanied by organ function or organic damage, such as the heart, brain, and kidney, and is the main risk factor of cardio-cerebrovascular disease [11, 12]. It interacts with renal diseases. On the one hand, when the patient's blood pressure is not controlled and treated in a timely and correct

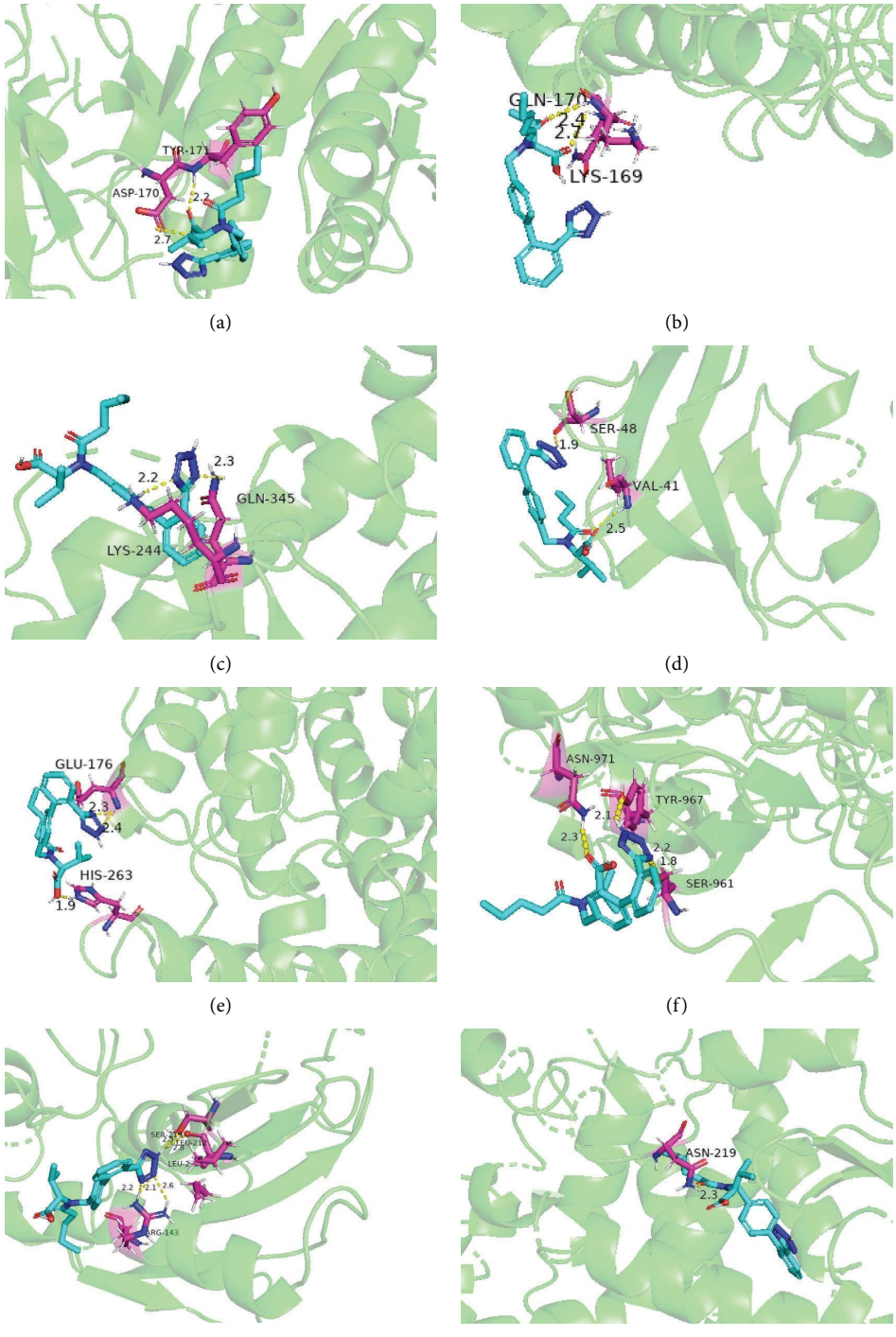

Figure 3: Continued.

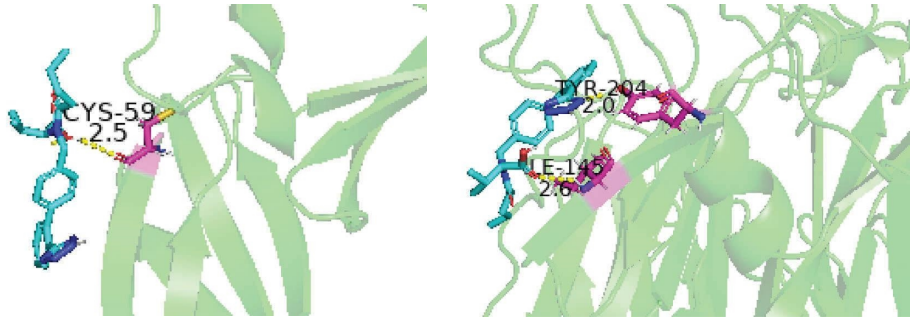

Figure 3: Molecular docking results (purple is the docking part). (a) Valsartan and EGFR; (b) valsartan and PTGS2; (c) valsartan and PPARG; (d) valsartan and ERBB2; (e) valsartan and ACE; (f) valsartan and STAT3; (g) valsartan and MMP9; (h) valsartan and PPARA; (i) valsartan and PTPRC; (j) valsartan and ITGB1.

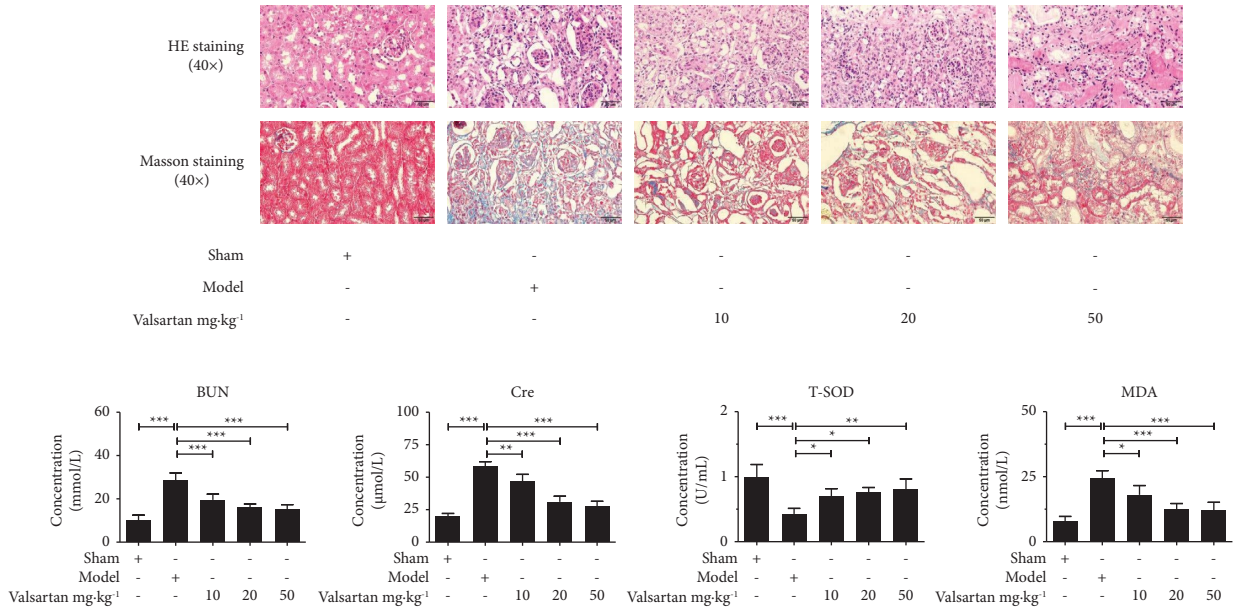

Figure 4: Changes in renal pathology, serum BUN, Cre, T-SOD, and MDA levels in each group. Note: compared with the model group, $^{*}P < 0.05$, $^{**}P < 0.01$, and $^{***}P < 0.001$.

manner, it leads to insufficient blood supply to the kidneys, causing damage to renal function and creating chronic renal failure [13, 14]. On the other hand, renal parenchymal lesions and renal artery lesions can increase blood pressure, forming hypertension [15, 16]. Therefore, attention must be paid to the interaction between hypertension and renal function damage, which is of great significance to formulate a reasonable and effective treatment plan.

Various studies have shown that the progression of CKD from the mild to terminal stage can be delayed by controlling hypertension and proteinuria [17, 18], and valsartan can reduce blood pressure and aldosterone levels by blocking angiotensin II, reducing blood volume and sodium content in blood, improving renal function of CKD patients, and slowing disease progression [19–22], but the mechanism of valsartan in improving renal function has not been clarified.

In recent years, network pharmacology has been applied more and more in drug development, which checks predicted targets of compounds with predicted targets of disease, along with further analyses of the potential mechanism of this compound in treating disease by constructing a network map of "drug-key target-disease" [23, 24]. In this study, we conducted a systematic analysis of the potential mechanism of valsartan in treating chronic renal failure using a network pharmacology approach. We identified 10 key genes affected by valsartan in chronic renal failure, including epidermal growth factor receptor (EGFR), cyclooxygenase 2 (PTGS2), peroxisome proliferator-activated receptor γ (PPARG), tyrosine kinase receptor 2 (ERBB2), angiotensin-converting enzyme (ACE), signal transduction and transcription activator protein 3 (STAT3), matrix metalloproteinase 9 (MMP9), peroxisome proliferator-activated receptor α (PPARA), protein tyrosine

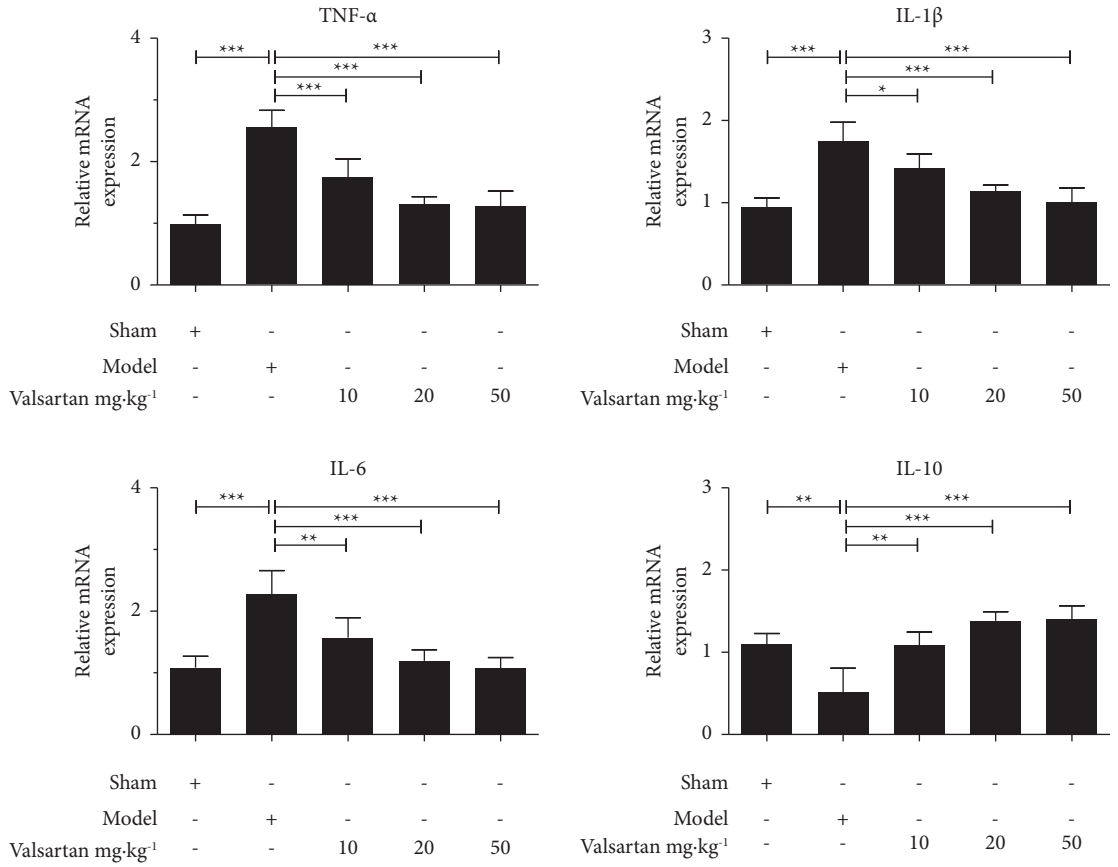

Figure 5: Expression of inflammatory cytokines in renal aspects of each group. Note: compared with the model group, $^{**}P < 0.01$ and $^{***}P < 0.001$.

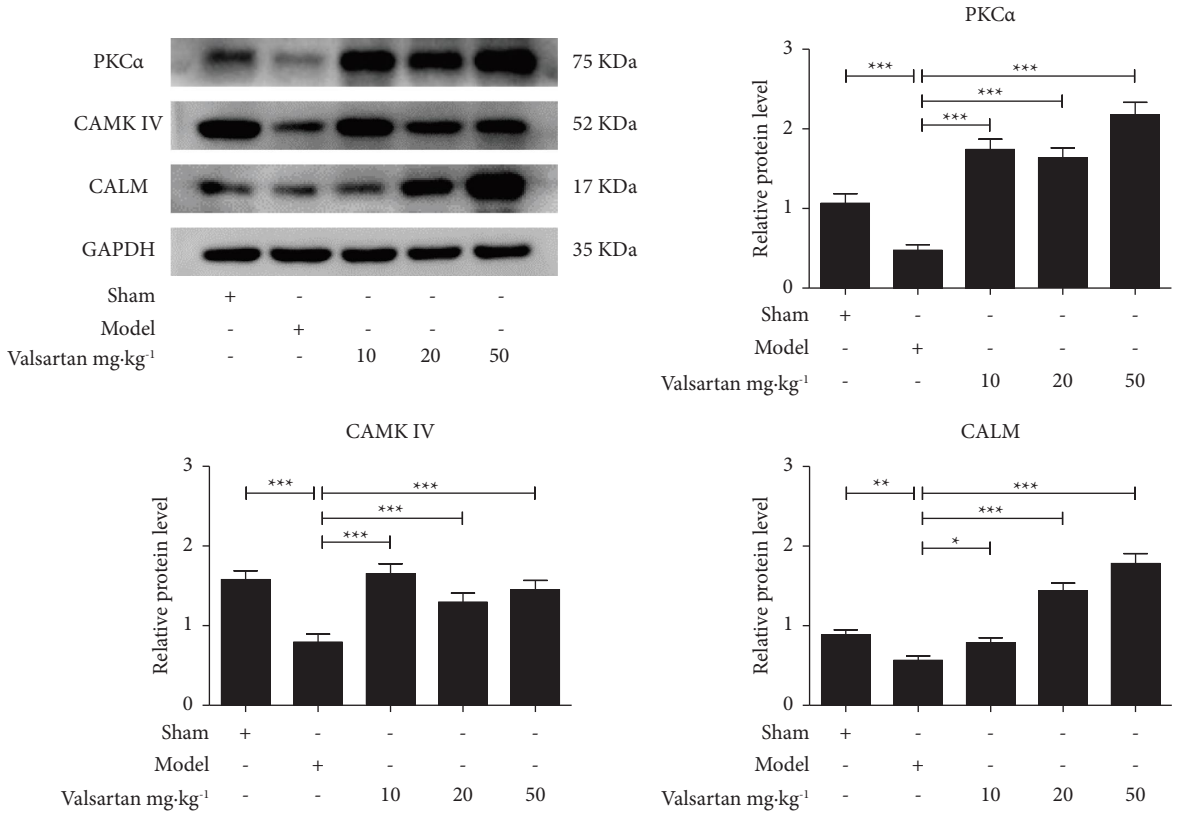

Figure 6: Expression of protein in renal tissue of each group. Note: compared with the model group, $^{*}P < 0.05$, $^{**}P < 0.01$, and $^{***}P < 0.001$.

phosphatase receptor C (PTPRC), and integrin β 1 (ITGB1). KEGG enrichment analysis predicted that valsartan primarily exerts its effects through the following pathways: neuroactive ligand-receptor interaction, calcium ion signaling pathway, hypoxia-inducible factor 1 signaling pathway, cancer signaling pathways (including proteoglycans in cancer, PD-L1 expression, and the PD-1 checkpoint pathway in cancer), cell fluid shear stress, atherosclerosis, and cyclic adenylate signaling pathway (cAMP signaling pathway). The results of molecular docking demonstrate a favorable binding interaction between valsartan and the core targets, with binding energies of −3.14, −2.77, −2.6, −3.31, −1.48, −1.52, −4.43, −1.09, −2.08, and −2.41 kcal/mol, respectively. This indicates that valsartan may potentially exert a therapeutic effect on chronic kidney failure through modulation of the aforementioned target proteins. Previous studies have revealed that the epidermal growth factor receptor (EGFR) and ErbB2 play a role in enhancing proliferative capacity and promoting cell survival. ErbB receptors could interact with the Ca^{2+}-sensor and transducer protein calmodulin (CaM) directly, by phosphorylation of the receptors via CaM-dependent kinases, and regulate their activity and functions [25]. In addition, PTGS2 as an enzyme complex plays an important role in the conversion of arachidonic acid to prostaglandins, and some research shows that CaMKII acts as an upstream cascade to facilitate its transcription and expression; it indicates that PTGS2 may be related to the calcium signaling pathway [26]. Given the complexity of the hub target molecular docking results and KEGG enrichment analysis, the subsequent experiments in this study verified the mechanism of valsartan in treating chronic renal failure through the calcium signaling pathway.

This study showed that valsartan, compared with the model group, significantly improved the glomerular and renal interstitial structure, reduced renal collagen fiber deposition, alleviated the degree of renal fibrosis, and significantly reduced serum Cre, BUN, and MDA while increasing T-SOD in mice with chronic renal failure ($P < 0.05$) (Figure 4). In addition, it can improve the degree of inflammation in the kidneys and reduce the mRNA expression levels of TNF-α, IL-1β, IL-6, and elevated IL-10 ($P < 0.05$) in mouse kidney tissue (Figure 5). The WB assay showed that valsartan could significantly upregulate protein expression levels of CALM, PKCα, and CaMKIV in renal tissue ($P < 0.01$ or $P < 0.001$) (Figure 6), as valsartan could improve chronic renal failure through activation of calcium ion signaling along with dose dependence.

In conclusion, by combining network pharmacology methods and construction of the "valsartan-target-chronic renal failure" network, specific targets and mechanisms of valsartan on chronic renal failure were obtained. The possible mechanism of valsartan in improving chronic renal failure was preliminarily explored, which may provide a new solution to treat chronic renal failure. Yet, due to numerous pathways and complex mechanisms in chronic renal failure, this must be further studied to learn if valsartan also improves chronic renal failure through other action mechanisms.

Data Availability

The data that support the findings of this study are available from the corresponding author upon reasonable request.

Conflicts of Interest

The authors declare that there are no conflicts of interest regarding the publication of this article.

Acknowledgments

This work was supported by the Anhui Provincial Natural Science Foundation Project (2108085MH255) and the Xuancheng Municipal-Level Science and Technology Plan Project (1812).

References

[1] L. X. Zhang and L. Zuo, "Current burden of end-stage kidney disease and its future trend in China," *Clinical Nephrology*, vol. 86, no. S1, pp. S27–S28, 2016.

[2] A. K. Bello, A. Levin, M. Tonelli et al., "Assessment of global kidney health care status," *JAMA*, vol. 317, no. 18, pp. 1864–1881, 2017.

[3] T. Tanaka, S. Miura, M. Tanaka, Y. Uehara, T. Hirano, and K. Saku, "Efficacies of controlling morning blood pressure and protecting the kidneys by treatment with valsartan and nifedipine CR or valsartan and amlodipine (MONICA study)," *Journal of Clinical Medicine Research*, vol. 5, no. 6, pp. 432–440, 2013.

[4] R. T. Gansevoort, R. Correa-Rotter, B. R. Hemmelgarn et al., "Chronic kidney disease and cardiovascular risk: epidemiology, mechanisms, and prevention," *The Lancet*, vol. 382, no. 9889, pp. 339–352, 2013.

[5] A. S. Go, G. M. Chertow, D. Fan, C. E. McCulloch, and C. Hsu, "Chronic kidney disease and the risks of death, cardiovascular events, and hospitalization," *New England Journal of Medicine*, vol. 351, no. 13, pp. 1296–1305, 2004.

[6] G. Faa, A. Sanna, C. Gerosa et al., "Renal physiological regenerative medicine to prevent chronic renal failure: should we start at birth?" *Clinica Chimica Acta*, vol. 444, pp. 156–162, 2015.

[7] M. E. Stauffer and T. Fan, "Prevalence of anemia in chronic kidney disease in the United States," *PLoS One*, vol. 9, no. 1, Article ID e84943, 2014.

[8] L. S. Goodman, A. Gilman, and L. L. Brunton, *Goodman & Gilman's the Pharmacological Basis of Therapeutics*, McGraw-Hill, New York, NY, USA, 2006.

[9] F. Wu, H. Y. Wang, F. Cai et al., "Valsartan decreases platelet activity and arterial thrombotic events in elderly patients with hypertension," *Chinese Medical Journal*, vol. 128, no. 2, pp. 153–158, 2015.

[10] G. Qian, Y. Zhu, S. Tao et al., "Increased hemoglobin concentration and related factors in maintenance hemodialysis patients in Anhui,China," *Medicine (Baltimore)*, vol. 101, no. 46, Article ID e31397, 2022.

[11] D. T. Lackland and M. A. Weber, "Global burden of cardiovascular disease and stroke: hypertension at the core,"

Canadian Journal of Cardiology, vol. 31, no. 5, pp. 569–571, 2015.

[12] S. Mendis, P. Puska, and B. Norrving, *Global atlas on cardiovascular disease prevention and control*, Geneva World Health Organization, Geneva, Switzerland, 2011.

[13] A. V. Chobanian, G. L. Bakris, H. R. Black et al., "Seventh report of the joint national committee on prevention, detection, evaluation, and treatment of high blood pressure," *Hypertension*, vol. 42, no. 6, pp. 1206–1252, 2003.

[14] M. I. Perez and V. M. Musini, "Pharmacological interventions for hypertensive emergencies: a Cochrane systematic review," *Journal of Human Hypertension*, vol. 22, no. 9, pp. 596–607, 2008.

[15] Y. Sata, G. A. Head, K. Denton, C. N. May, and M. P. Schlaich, "Role of the sympathetic nervous system and its modulation in renal hypertension," *Frontiers of Medicine*, vol. 5, p. 82, 2018.

[16] H. Bartolomaeus, A. Balogh, M. Yakoub et al., "Short-chain fatty acid propionate protects from hypertensive cardiovascular damage," *Circulation*, vol. 139, no. 11, pp. 1407–1421, 2019.

[17] F. A. Holtkamp, D. de Zeeuw, P. A. de Graeff et al., "Albuminuria and blood pressure, independent targets for cardioprotective therapy in patients with diabetes and nephropathy: a post hoc analysis of the combined RENAAL and IDNT trials," *European Heart Journal*, vol. 32, no. 12, pp. 1493–1499, 2011.

[18] K. M. A. Ameen and M. A. Kashif, "To compare anti-albumin urea effects of valsartan alone with combination of valsartan and amlodipine in patients of chronic kidney disease," *Pakistan Journal of Medical Sciences*, vol. 32, no. 3, pp. 613–616, 2016.

[19] E. J. Lewis, L. G. Hunsicker, R. P. Bain, and R. D. Rohde, "The effect of angiotensin-converting-enzyme inhibition on diabetic nephropathy," *New England Journal of Medicine*, vol. 329, no. 20, pp. 1456–1462, 1993.

[20] E. J. Lewis, L. G. Hunsicker, W. R. Clarke et al., "Renoprotective effect of the angiotensin-receptor antagonist irbesartan in patients with nephropathy due to type 2 diabetes," *New England Journal of Medicine*, vol. 345, no. 12, pp. 851–860, 2001.

[21] S. Petch, E. O'Connor, A. McGrath, and S. Daly, "Valsartan exposure in pregnancy with resultant anhydramnios and chronic kidney disease in a late preterm infant," *BMJ Case Reports*, vol. 14, no. 5, Article ID e240810, 2021.

[22] A. Jankauskiene, D. Drozdz, A. Wasilewska et al., "Efficacy and safety of valsartan in children aged 1–5 years with hypertension, with or without chronic kidney disease: a randomized, double-blind study followed by open-label phase," *Current Medical Research and Opinion*, vol. 37, no. 12, pp. 2113–2122, 2021.

[23] C. Nogales, Z. M. Mamdouh, M. List, C. Kiel, A. I. Casas, and H. H. Schmidt, "Network pharmacology: curing causal mechanisms instead of treating symptoms," *Trends in Pharmacological Sciences*, vol. 43, no. 2, pp. 136–150, 2022.

[24] Y. Dong, Q. Zhao, and Y. Wang, "Network pharmacology-based investigation of potential targets of astragalus membranaceous-angelica sinensis compound acting on diabetic nephropathy," *Scientific Reports*, vol. 11, no. 1, Article ID 19496, 2021.

[25] A. Villalobo, "Regulation of ErbB receptors by the Ca2+ sensor protein calmodulin in cancer," *Biomedicines*, vol. 11, no. 3, p. 661, 2023.

[26] C. Y. Lai, M. C. Hsieh, Y. C. Ho et al., "GluN2B/CaMKII mediates CFA-induced hyperalgesia via HDAC4-modified spinal COX2 transcription," *Neuropharmacology*, vol. 135, pp. 536–546, 2018.